AIAA JOURNAL
Vol. 32, No. 8, August 1994

Noise Reduction Properties of a Multiple-Source Schlieren System

Steven H. Collicott* and Terry Ray Salyer†
Purdue University, West Lafayette, Indiana 47907

Schlieren images often contain noise that is caused by density gradients in the air that surrounds the wind-tunnel test section. It has been shown that multiple-source, or sharp-focusing, schlieren systems may reduce the region of space in which the schlieren system is most sensitive to density gradients. In this paper, the potential for noise reduction by minor modifications to traditional schlieren systems is examined. The modifications result in a multiple-source (sharp-focusing) schlieren system using the existing mirrors. Analysis shows that, for a system with an incoherent narrowband source, the imaging system, the slit spacing, and the transverse length scale of the noise govern the depth of focus. Also shown is that the maximum reduction of the noise scales linearly with the number of source slits.

I. Introduction

SCHLIEREN systems have long been used to visualize density fields in wind-tunnel research. A schlieren system is an imaging system with specialized illumination and aperture. The illumination is a collimated beam of light, and the unique feature of the aperture is a straight opaque cutoff, typically blocking half of the light in the Fourier transform plane. It is assumed that the reader is familiar with the elementary operating principles of the traditional schlieren system.[1]

Multiple-source, or sharp-focusing, schlieren systems were developed to eliminate one limitation of the traditional schlieren systems. This limitation is the fact that the schlieren system will detect density gradients not only in the wind tunnel but also in the region between the source slit and the knife edge. Thus, density gradients outside of the test facility will also contribute light and dark regions to the image. The multiple-source schlieren attempts to eliminate this image noise by probing the flow with a number of collimated beams in different directions. A multiple-source schlieren system with incoherent illumination can be viewed as the sum of a number of individual schlieren systems. The noise reduction effect is analyzed and described later.

"Sharp-focusing" is an unfortunate choice of modifiers to describe the system. Because a traditional schlieren system already focuses the object space (wind-tunnel model) into the image space, the term "sharp-focusing" does not convey any differences to the unenlightened. Thus "multiple-source schlieren" is a more descriptive name.

A. Motivation

Noise in schlieren images can arise from density gradients anywhere between the source slit and the knife edge. Examples of these density gradients are thermal currents in the room and turbulent boundary layers on the windows of the wind-tunnel test section. The severity of the noise depends not only on the magnitude of these superfluous density gradients but also on the magnitude of the density gradient that is to be visualized. As the Mach number of a blowdown facility increases, the density decreases, and thus density gradients decrease. Hence extraneous thermal currents that cause negligible noise in the image of a Mach 2 flow may obscure the signal in a higher Mach number facility.

To reduce the image noise, a multiple-source schlieren system superimposes images from a series of traditional schlieren systems. In place of a single source slit, a series of slits, or collectively the source grid, is used. In place of the traditional knife edge, a series of cutoff slits, or the cutoff grid, is used. For each source slit, there exists a corresponding cutoff slit. As implied by the name, the cutoff slits function analogously to the knife edge in a traditional schlieren. As sketched in Fig. 1, the centerlines of the beams are coincident at both the ideal (paraxial) object plane and the ideal (paraxial) image plane. Thus the images of the ideal object plane created by each individual schlieren system coincide at the ideal image plane. The key to the operation of the multiple-source schlieren[2–6] is simply that the centerlines of the beams are not coincident in the remainder of the region between the source and cutoff slits. This causes the individual images of planes outside the ideal object plane to not be coincident in the ideal image plane. The shift between the various images of objects in planes other than the ideal object plane results in reduced visibility of the image of that object. The further a disturbance is from the ideal object plane, the more the images are spread out in the image plane. Although a given disturbance now affects a larger region of the image plane, the magnitude of the effect at any one point is diminished. Thus the multiple-source schlieren possesses a certain degree of axial selectivity. This depth of field is a property of imaging systems in general and is not unique to this application.

B. Review of Previous Work

Previous work in multiple-source schlieren systems apparently began about 1950.[2–4] This initial period of interest is terminated by probably the most comprehensive analysis to date, an MIT Master's thesis by Boedeker in 1959.[5] The thesis is a mixture of the geometric analyses of traditional schlieren operation and depth of focus in an imaging system. Boedeker's approach is used to compare several different multiple-source schlieren systems. Boedeker addresses the depth of focus of an imaging system with a point object, but the results do not appear to apply directly to multiple-source schlieren systems for viewing finite-sized objects. Other papers of the era of initial interest[2–4] are briefly compared with Boedecker's. These papers describe the basic operation in a qualitative manner. The descriptions are useful for acquiring an insight into the device and its operation but are insufficient for noise reduction design purposes. Because the initial era precedes the invention of the laser, use of a highly coherent light source was not considered. One report following this era reports on the merging of multiple-source and color schlieren designs.[7]

Presented as Paper 93-2917 at the AIAA 24th Fluid Dynamics, Plasmadynamics, and Lasers Conference, Orlando, FL, July 6–9, 1993; received Aug. 4, 1993; revision received Dec. 27, 1993; accepted for publication Dec. 27, 1993.

*Assistant Professor, School of Aeronautics and Astronautics, 1282 Grissom Hall.

†Graduate Student, School of Aeronautics and Astronautics, 1282 Grissom Hall.

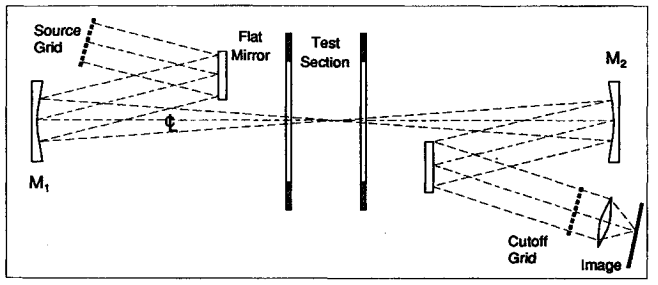

Fig. 1 Multiple-source schlieren system with mirrors.

The present era of interest in focusing schlieren has grown from work performed by Weinstein[6] at NASA Langley Research Center beginning in the late 1980s. Some new analysis is found in this paper, and it describes several of a wide variety of multiple-source schlieren systems which he has demonstrated. Weinstein's work has created interest in the multiple-source systems by other researchers,[8,9] including the present authors.

Most papers from both eras primarily describe how to maximize the field of view without recourse to large mirrors. Some papers discuss aberrations as an intrinsic property of a lens, independent of the application in which it is used. This is an improper description; aberrations are approximate measures of imaging performance determined by both the lens and the geometry in which it is used.

C. Goal of This Work

The goal of this work differs from the goals of previous analyses. The goal is to determine the noise reduction capabilities of multiple-source modifications to an existing schlieren system. Sources of noise can include, for example, thermal currents from compressors in the room, warm and cool drafts through doors and ventilation, and cooling fans for electronics. Application of the previous analytical efforts did not provide a sound method to design a multiple-source schlieren system or to quantitatively predict its noise reduction performance. Therefore, analysis of the axial selectivity of multiple-source schlieren systems was performed. The present work defines a practical quantitative measure of the axial selectivity and then determines how this is governed by system parameters. This permits design and analysis of focusing schlieren systems for noise reduction in the schlieren images from supersonic wind tunnels. Prediction of integration length, including the minimum possible integration length, is also possible with the results of the analysis.

II. Analysis

Fourier optics analysis generally fails when applied to incoherent light transilluminating an object at different angles. Effects of pure phase objects, such as shock waves and expansion fans, in an incoherent system also fail to be described well by Fourier optics. Complicating analysis further is the presence of the knife edge or cutoff grid. These cutoff devices permit visualization of the density gradient field, but by doing so, they destroy the linearity in intensity of an incoherent system. Thus a more comprehensive analysis method is required. Description of the light by use of the mutual intensity function is sufficient to describe incoherent illumination at arbitrary angles, the effect of pure phase objects, and the propagation through the optical system.[10] A small density gradient model is examined to determine the minimum possible integration length and its dependence on slit size, spacing, and quantity.

A. Geometric Analysis

The multiple-source schlieren system can be regarded as a combination of a series of individual schlieren systems, or it can be considered as an imaging system with a unique extended source and a corresponding aperture. For an incoherent source, this combination occurs by a summing of the individual image intensities. For partially or fully coherent sources, the combination is more complex and is not addressed here. It is assumed that a typical schlieren system has a source slit small enough such that the depth of focus of the system is greater than the total system length. This is a safe assumption because the necessary sensitivity of a schlieren system requires a small source slit.[1]

Images of objects outside of the ideal object plane fail to coincide in the ideal image plane of the multiple-source system. Three example images formed from different object positions are sketched in the three columns of Fig. 2. The axial selectivity is best described by considering the distance from the ideal object plane at which a disturbance in the density field has individual images completely displaced from each other (such as the left column of Fig. 2). That distance is the value of $\tilde{z}_0 - z_0$, which causes $h = ML_f$, where M is the imaging magnification, and L_f is the transverse length scale of the disturbance in the object space. Call twice this value (for both sides of the object plane) the integration length L_i. This definition differs from Boedeker's since it depends on the length scale of the object, which is necessary to arrive at an accurate description of the axial selectivity. For an interbeam angle of α, it can be seen that, for small α,

$$L_i = 2L_f/\tan(\alpha) \approx 2L_f/\alpha \tag{1}$$

Note that the axial selectivity depends only on the interbeam angle and the length scale of the disturbance. Thus different length scales in the fluid are selected differently. This is consistent with the depth of focus in an imaging system.[11]

B. Mutual Intensity Analysis

Fourier optics describes the amplitude of the electric field and the intensity in a series of transverse planes, for example, an object plane and an image plane. Similarly, a quantity termed the mutual intensity may be defined in these transverse planes. The mutual intensity function is defined to be the time-averaged product of the electric field amplitude at point P_1 and the conjugate of the field at point P_2:

$$J(P_1, P_2) = [U(P_1)U^*(P_2)] \tag{2}$$

Note that, for $P_1 = P_2$, the mutual intensity function describes the intensity at the point P_1. Propagation of the mutual intensity through thin phase objects, lenses, and free space is described by methods analogous to Fourier optics, but in four dimensions rather than two.[10]

To apply these tools to the multiple-source schlieren system, a description of the mutual intensity incident on the wind-tunnel test section is required. The multiple-source schlieren system has source slits, beam angles, and cutoff slits that are a function of only one transverse direction, say x. In the y-z plane, the system acts like a simple incoherent imaging system. This is consistent with the x-y separability of the functions that describe the source slits, lenses and mirrors, cutoff slits, and the separability of the free-space propagation integrals. Thus $J(x_1, y_1; x_2, y_2) = J_x(x_1; x_2)$

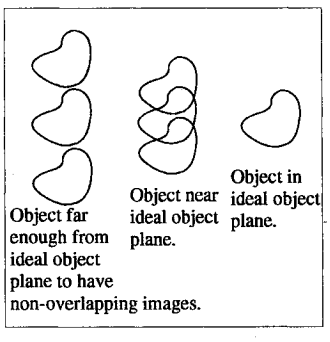

Fig. 2 Offset of individual schlieren images caused by the angle between beams.

$J_y(y_1; y_2)$, and the present task is to solve for the propagation of the J_x factor.

The mutual intensity for incoherent illumination of the source slits is described by

$$J_x(x_1;\ x_2) = \sum_{i=-N}^{N} \text{rect}\left(\frac{x_1 - ia_2}{a_0}\right)\delta(x_1 - x_2) \tag{3}$$

where a_0 is the slit width, and a_2 is the distance between centerlines of adjacent slits. The rect function is defined to be

$$\begin{aligned} \text{rect}(x) &= 1 \text{ for } |x| < 1/2 \\ &= 1/2 \text{ for } |x| = 1/2 \\ &= 0 \text{ for } |x| = 1/2 \end{aligned} \tag{4}$$

At the paraxial object plane, the mutual intensity is, ignoring a leading constant, a two-dimensional Fourier transform[10] of J_x,

$$J_{\text{obj}}(u_1;\ u_2) = \text{sinc}\left[\frac{a_0}{\lambda_f}(u_1 - u_2)\right]\sum_{i=-N}^{N} \exp\left[j2\pi\,\frac{i\sin\alpha}{\lambda}(u_1 - u_2)\right] \tag{5}$$

The reader may verify by setting $u_1 = u_2$ that this is a uniform intensity field. The sinc function is the Fourier transform of the rect function and is defined to be $\text{sinc}(x) = \sin(\pi x)/(\pi x)$.

The object that this mutual intensity passes through in aerodynamics research is a compressible flow. The density gradients in this field bend the light rays or, equivalently, deform the wave fronts. The purpose of this analysis is to determine how the multiple-source schlieren system reacts to density gradients located anywhere between the mirrors. To produce an analytical model that is soluble and remains relevant, the concept of an "effective transparency" approximation is introduced. This approximation is used to model density changes outside the ideal object plane, thereby avoiding the complications of computing the mutual intensity at planes that are not conjugate planes or Fourier transform pairs. The effective transparency is assumed to be the object plane transparency that has the out-of-plane disturbance replicated and shifted as each beam would carry it to the object plane. This is sketched in Fig. 3 for a series of five beams. No diffractive effects of propagation are included, which is not likely to be a problem because of the large depth of focus of each individual schlieren system.

A localized phase disturbance at the point $(x, z) = (x_D, -L_D)$ in an otherwise uniform density field can be written as an amplitude transmittance for the ith beam: $t_i(x) = \exp[j2\pi b\delta(x - \tilde{x})]$. The shift $\tilde{x}$ is determined from geometry (Fig. 3), $\tilde{x} = x_D - ia_2L_D/f$. For small phase disturbances, $b \ll 1$, and $t_i(x)$ is approximated by the first two terms of the Taylor series, $t_i(x) \approx 1 + j2\pi b\delta(x - \tilde{x})$. Mutual intensity is modified by a thin transparency[10] according to

$$J_{\text{out}}(x_1, y_1; x_2, y_2) = J_{\text{in}}(x_1, y_1; x_2, y_2)t(x_1, y_1)t^*(x_2, y_2) \tag{6}$$

The product of $t(u_1)$ and $t^*(u_2)$ is

$$t_i(u_1)t_i^*(u_2) \approx 1 + j2\pi b[\delta(u_1 - \tilde{x}) - \delta(u_2 - \tilde{x})] + (2\pi b)^2\delta(u_1 - \tilde{x})\delta(u_2 - \tilde{x}) \tag{7}$$

It can be shown that the second term does not contribute to the output plane intensity. This and the linearity (in mutual intensity) of the propagation integrals permit analysis to proceed with

$$t_i(u_1)t_i^*(u_2) \approx 1 + (2\pi b)^2\delta(u_1 - \tilde{x})\delta(u_2 - \tilde{x}) \tag{8}$$

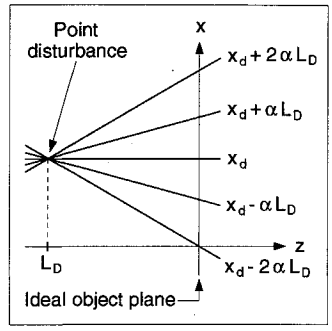

Fig. 3 Lengths and angles that are used to define the effective transparency.

This results in J'_{obj}, the mutual intensity after the object plane,

$$J'_{\text{obj}}(u_1; u_2) = \text{sinc}\left[\frac{a_0}{\lambda_f}(u_1 - u_2)\right] \times \left[1 + (2\pi b)^2\sum_{i=-N}^{N}\delta(u_1 - \tilde{x})\,\delta(u_2 - \tilde{x})\right] \times \sum_{i=1}^{N}\exp\left[j2\pi\,\frac{i\sin\alpha}{\lambda}(u_1 - u_2)\right] \tag{9}$$

The product of summations is the portion of interest. The other part represents a uniform transparency that will produce a uniform intensity in the output plane, and so it is of little interest here. Thus $J'_{\text{obj}} = J_{\text{unif}} + J_p$, where J_p is the perturbation mutual intensity. The perturbation mutual intensity is a summation of the individual beam perturbations, or

$$J_p(u_1; u_2) = \sum_{i=-N}^{N} J_{pi}(u_1; u_2) \tag{10}$$

where the individual beam perturbation mutual intensities are, from Eq. (9),

$$J_{pi}(u_1; u_2) = (2\pi b)^2\,\text{sinc}\left[\frac{a_0}{\lambda_f}(u_1 - u_2)\right]\delta(u_1 - \tilde{x})\,\delta(u_2 - \tilde{x}) \times \exp\left[-j2\pi\,\frac{i\sin\alpha}{\lambda}(u_1 - u_2)\right] \tag{11}$$

The imaging system processes this input perturbation mutual intensity in the x-z plane according to a two-dimensional superposition integral, resulting in the output plane perturbation intensity

$$I_{pi}(\bar{x}) = \int_{-\infty}^{\infty}\int_{-\infty}^{\infty} J_{pi}(u_1; u_2)K(\bar{x}, u_1)K^*(\bar{x}, u_2)\,du_1\,du_2 \tag{12}$$

The scaled and reversed output plane dimension is $\bar{x} = -Mx$. The amplitude spread function $K(\bar{x}, u)$ is given by a Fourier transform of the pupil function.[10] For the layout of the schlieren, and ignoring a leading constant, this relation is

$$K(\bar{x}, u) = \exp\left(j\frac{\pi d}{\lambda f^2}\bar{x}^2\right)\int_{-\infty}^{\infty} P(\xi)\exp\left[-j\,\frac{2\pi}{\lambda f}(u - \bar{x})\,\xi\right]d\xi \tag{13}$$

For each source and cutoff slit pair in either a traditional or a multiple-source schlieren, the pupil function $P(\xi)$ is determined by

both the bandwidth of the illumination and the cutoff slit, as sketched in Fig. 4. Thus the pupil function is a rect function with a width that depends on the source slit width, the portion of the image of the source slit cut by the cutoff grid, and, to some extent, the deflection of rays by density gradients. In this work it has already been assumed that $b \ll 1$, and so the deflection due to density gradients is neglected. These assumptions produce a pupil function for the ith beam that is, with reference to Fig. 4,

$$P_i(\xi) = \text{rect}\left(\frac{\xi - ia_2 - a_3}{a_0 - a_3}\right) \tag{14}$$

Substitution of this into Eqs. (12) and (13) results in the output plane perturbation intensity, again ignoring leading constants,

$$I_p(x) = \sum_{i=-N}^{N} \text{sinc}^2\left[\frac{a_0 - a_3}{\lambda f_2}\left(x - Mx_d - i\frac{ML_d\alpha a_2}{f}\right)\right] \tag{15}$$

Here f_2 is the focal length of the lens following the cutoff grid. Because the grid is in the Fourier transform plane of the second mirror, one more Fourier transform is required to produce the final image. As long as the F-number of this lens is smaller than that of the mirror, the lens will pass all of the light that passes the grid. Thus no aperture effects are introduced. In this afocal imaging design, the magnification is then $M = f_2/f$. The perturbation intensity is approximately the distribution of intensity in the image plane caused by a small disturbance at a general location in the object space.

Note that when this expression is applied to the traditional schlieren ($N = 0$), it reduces to

$$I_p|_{(N=0)} = \text{sinc}^2\left[\frac{a_0 - a_3}{\lambda f_2}(x - Mx_d)\right] \tag{16}$$

The dependence on L_d has disappeared, demonstrating that a disturbance anywhere between the source slit and knife edge will be detected.

To simplify interpretation of the perturbation intensity in the multiple source schlieren, set $x_d = 0$ and let L_d remain general. This constrains the model to considering density disturbances on the optical axis. A nonzero x_d simply shifts the response up or down. Let us further assume that $a_3 = a_0/2$, which means that each slit in the cutoff grid cuts half of the image of the corresponding source slit. This is not unusual for traditional schlierens and appears reasonable for the multiple-source schlieren. The value of $(a_0 - a_3)$ and the integration length are inversely proportional, and so it is simple to reproduce the following work for other values of a_3. With these assumptions, the perturbation intensity is reduced to

$$I_p(x) = \sum_{i=-N}^{N} \text{sinc}^2\left[\frac{a_0}{2\lambda f_2}(x - i\alpha ML_d a_2/f)\right] \tag{17}$$

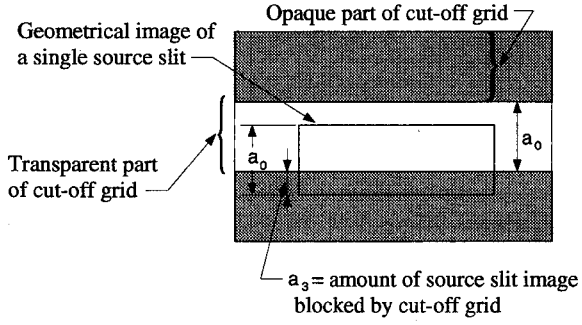

Fig. 4 Length scales in the plane of the cutoff grid. Grid-to-grid magnification is unity because of the symmetry of the mirrored schlieren system.

This expression is plotted vs x and L_d for $N = 5$ (11 slits) in Fig. 5. In this plot, $L_d = 0$ at the left and increases to the right; $x = 0$ along the back and increases toward the front. The figure shows one quarter of the response for a system of 11 pairs of source and cutoff slits. The symmetry of the response in both L_d and x permits examination of just one quarter. The peak at the left rear of the plot shows that the system responds best to a density disturbance in the ideal object plane. This is good news; some axial selectivity has been created.

Several features of this plot besides the central peak should be noted because they exist in the perturbation intensities for all numbers of slits. The walkoff of the individual squared sinc functions is analogous to the walkoff of individual images of a fluid disturbance discussed in the geometrical section. This tells us that the shortest possible integration length is governed not by the fluid length scales but by the diffractive response of the optical system itself. Thus the minimum integration length may be considered to be

$$(L_i)_{\min} = \frac{4\lambda f}{\alpha a_0} = \frac{4\lambda f^2}{a_0 a_2} \tag{18}$$

The second item to note is that the response never goes to zero for any value of L_d. This is shown in Fig. 5, where the central left-to-right ridge is 1/11 of the strength of the peak response. This ridge represents the response of the central pair of source and cutoff slits (a simple schlieren system with no axial selectivity). Note the similar ridges for each pair of source and cutoff slits. This is another manifestation of the system acting as a summation of individual schlieren systems. Thus, although the integration length may be shortened, the response of the schlieren system to density disturbances throughout the system is not eliminated but reduced to a value of $1/(2N + 1)$ of the peak. For example, a single order of magnitude reduction requires only $N = 5$ slits on either side of the center slit, for a total of 11 slits. Then the desired integration length and the relevant length scale, fluid or optical, for the purpose at hand are used to specify the interbeam angle. The interbeam angle multiplied by $2N$ gives the maximum included angle. Because $2N\alpha < 2 \tan^{-1}(0.5/F^{\#})$ for an optical system, there is always a tradeoff between the reduction of the integration length and the magnitude of the noise reduction.

III. Experiment

A single-source schlieren system is modified to have three source slits. This system has some noise reduction capabilities, and it produces images in which key points of the preceding analysis are easily observed. The three source slit system is as shown in

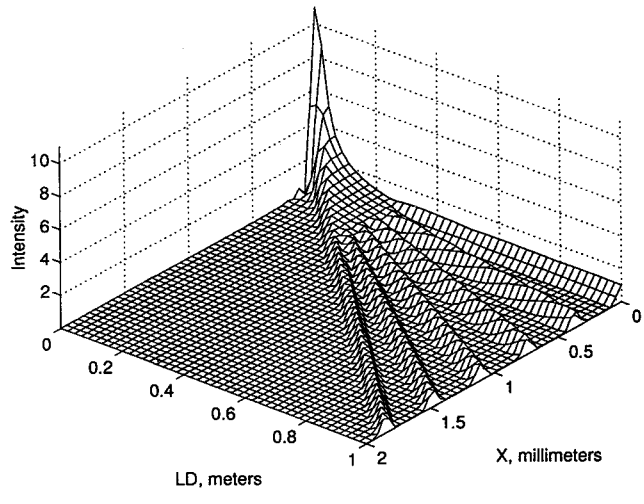

Fig. 5 Intensity response of an 11-slit schlieren to a point noise at different distances from the test section. Left edge is the tunnel centerline. The angle between ridges is the interbeam angle α.

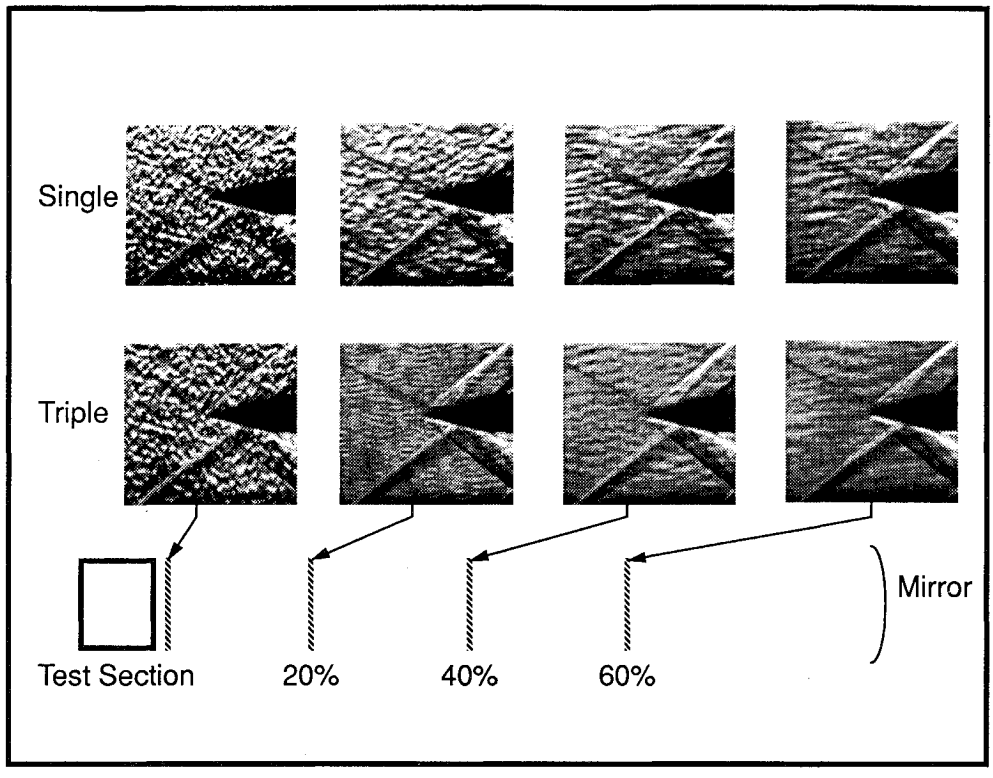

Fig. 6 Images from single- (top row) and triple-source (bottom row) schlieren systems for four noise inputs. Images in a column are acquired with identical noise input to the system. Flow is from left to right at Mach 2.5.

Fig. 1. The distance between slits is 6 mm, and each slit is 1.5 mm wide. The focal length of the F/10 spherical mirrors is 1.52 m, and the imaging lens after the cutoff grid is F/3 with a focal length of 200 mm. The images are recorded on a charge-coupled device array with 512 pixels across and 480 pixels high and a 7-bit gray scale.

To observe the noise reduction capabilities of the system, a consistent source of noise is required. A noise mask is created by exposing a holographic plate to a speckle pattern of 3-mm length scale. The holographic plate is developed and bleached to change the pattern into a phase disturbance. The phase disturbance of the bleached speckle pattern simulates thermal currents of the same length scale.

Figure 6 presents eight images that demonstrate the noise reduction capability of the three source schlieren system. The slits are horizontal in these photographs, and the flow is to the right at Mach 2.5. The top row of images are produced by a single-source schlieren system. The bottom row of images are from the triple-source schlieren system. The two images that make up a column are acquired with identical noise in the system, and the noise is located differently for the four columns. In the first, or leftmost, column, the noise mask is placed immediately outside the test section. In the second through fourth columns, the noise mask is located at 20, 40, and 60%, respectively, of the distance between the test section and the spherical mirror. The noise mask is made to be strong enough to obscure shock waves in this Mach 2.5 flow, as may actual noise in some hypersonic facilities. Because of the greater density in this facility, the noise mask is also strong enough to slightly, but noticeably, blur the edges of the wedge.

The images in the first column of Fig. 6 show that the triple-source schlieren system detects noise near the test section in a manner similar to that of the single-source schlieren. The attached bow shocks from the wedge are barely visible, and the speckle pattern is clearly visible throughout the field. This is the response to noise within the "integration length" of the systems.

The second column contains images for the case with the noise introduced approximately 20% of the distance from the test section to the mirror. The noise reduction by the triple-source schlieren is dramatic; the lower image is unarguably far superior to the upper image. The bow shocks are clearly visible, as are an assortment of shock and Mach waves from wall defects in the test section. Note too that the expansion fans at the end of the wedged section of the body are clearly visible. As discussed in the analysis, there remains some residual response to the noise. This is evident as the wavelike background pattern throughout the lower image of the second column.

The third column shows a very clear image from the triple-source schlieren and even a little noise reduction in the single-source schlieren. The noise reduction in the single source is from the length of the source slit in the horizontal dimension. An extended source in a schlieren certainly will provide good depth of focus, but with near-zero sensitivity. Thus the source slits may only be long in one direction. Note in the lower image that the structure of the residual noise is different in the second and third columns. This is because the overlappings of speckle images from each source slit have different shifts for the two columns.

Images in the fourth, or rightmost, column are from noise placed 60% of the distance from the test section to the mirror. It is worth noting that the noise appears comparable or a little stronger in these images than in the images of the third column. The noise mask at this 60% point is actually in the beam path twice: once as the light travels from the test section to the mirror, and once as the reflected light travels off axis from the mirror to the cutoff grid. Thus noise reduction is doubly important when thermal currents exist in this region of the system. The size of this double ray path region can easily be found from a quick sketch of the beam paths.

An overall examination of the eight images shows that very few sources are required to achieve a substantial noise reduction for shock wave visualization. Noise reduction is also noticeable in the uniform flow region. The triple-source schlieren images are superior to those from the single-source schlieren for all conditions except noise very close to the test section. Noise close to the test section (within the integration length) is detected comparably by both systems.

IV. Conclusions

Analysis of multiple-source modifications to the existing schlieren system is presented to provide quantitative tools for

noise reduction design. Extension of the analysis to other geometries is simple, and as such the analysis is a basis for design of multiple-source schlieren systems. Image data are presented for direct comparison of single and multiple slit systems with identical noise inputs at various locations. The data are believed to be the most direct and comprehensive comparison of the two systems published to date. Further research is defining measures of noise reduction and shock visibility to provide a solid and quantitative reference for use in the design of multiple-source schlieren systems.

Reduction of the integration length is described quantitatively for small disturbances. Integration length depends linearly on the length scale of the disturbance and inversely on the tangent of the interbeam angle. The fundamental behavior of the optical system is shown, for the narrowband incoherent small disturbance case, to be a scalar summation of the intensities produced by individual schlieren systems. It is interesting to note that this result is similar to the result one could obtain from geometric optics analysis. However, the result obtained with the mutual intensity analysis provides the additional information about the minimum possible integration length as determined by diffractive effects.

Because integration length depends on the length scale of the object of interest, there is no single value of integration length for a multiple-source schlieren system. That is, the characteristics of the flow affect the value. It is easier to mitigate the noise from disturbances of small extent than from broad disturbances. Noise sources located outside the integration length (for the appropriate length scale) are reduced by a factor of $(2N + 1)$, the total number of source slits. The noise is not eliminated but is attenuated and spread out. An existing schlieren system is modified to have three slits. This system is shown to have noise reduction capabilities that, qualitatively, are substantial. Future work will quantify the noise reduction to further aid in design of such modifications to existing systems.

To design multiple-source schlieren modifications for noise reduction, one must know the length scale of the noise to be eliminated. The desired integration length and the mirror focal length will determine the separation between the source slits. The number of slits will determine the maximum attenuation. The requirements of reducing integration length and maximizing the noise reduction are shown to be conflicting. An improvement in one capability causes a deterioration in the other. Thus, each incoherent multiple-source schlieren system is a compromise between the two goals.

Acknowledgments

This research was supported through the 1992 Air Force Office of Scientific Research (AFOSR) Summer Faculty Program, under the direction of George Seibert of the Wright Labs. Experimental portions of the work were supported by the 1993 AFOSR Summer Research Extension Program Subcontract 93-144.

References

[1]Liepmann, H. W., and Roshko, A., *Elements of Gas Dynamics*, Wiley, New York, 1957.

[2]Burton, R. A., "A Modified Schlieren Apparatus for Large Areas of Field," *Journal of the Optical Society of America*, Vol. 39, No. 11, 1949, pp. 907, 908.

[3]Fish, R. W., and Parnham, K., "Focusing Schlieren Systems," ARC, Royal Aircraft Establishment, England, UK, TR IAP 999, Nov. 1950.

[4]Kantrowitz, A., and Trimpi, R. L., "A Sharp-Focusing Schlieren System," *Journal of Aeronautical Science*, Vol. 17, No. 5, 1950, pp. 311–314.

[5]Boedeker, L. R., "Analysis and Construction of a Sharp Focusing Schlieren System" Master's Thesis, Dept. of Aeronautics and Astronautics, Massachusetts Inst. of Technology, Cambridge, MA, 1959.

[6]Weinstein, L. M., "Large-Field High-Brightness Focusing Schlieren System," *AIAA Journal*, Vol. 31, No. 7, 1993, pp. 1250–1255.

[7]Rotem, Z., Hauptmann, E. G., and Claassen, L., "Semifocusing Color Schlieren System for Use in Fluid Mechanics and Heat Transfer," *Applied Optics*, Vol. 8, No. 11, 1969, pp. 2326–2328.

[8]Gartenburg, E., Weinstein, L. M., and Lee, E. E., Jr., "Aerodynamic Investigation with Focusing Schlieren in a Cryogenic Wind Tunnel," AIAA Paper 93-3485, July 1993.

[9]Price Cook, S., and Chokani, N., "Quantitative Results from the Focusing Schlieren Technique," AIAA Paper 93-0630, Jan. 1993.

[10]Goodman, J. W., *Statistical Optics*, Wiley, New York, 1985.

[11]Kingslake, R., *Optical System Design*, Academic Press, New York, 1983.